JARO 13: 505–515 (2012)
DOI: 10.1007/s10162-012-0329-0

JARO
Journal of the Association for Research in Otolaryngology

Research Article

Effects of Repeated "Benign" Noise Exposures in Young CBA Mice: Shedding Light on Age-related Hearing Loss

Yong Wang[1] and Chongyu Ren[1]

[1]*Division of Otolaryngology and Program in Neuroscience, University of Utah, 30 North, 1900 East, Salt Lake City, UT 84132-0002, USA*

Received: 10 September 2010; Accepted: 28 March 2012; Online publication: 25 April 2012

ABSTRACT

Temporary hearing threshold shift (TTS) resulting from a "benign" noise exposure can cause irreversible auditory nerve afferent terminal damage and retraction. While hearing thresholds and acute tissue injury recover within 1–2 weeks after a noise overexposure, it is not clear if multiple TTS noise exposures would result in cumulative damage even though sufficient TTS recovery time is provided. Here, we tested whether repeated TTS noise exposures affected permanent hearing thresholds and examined how that related to inner ear histopathology. Despite a peak 35–40 dB TTS 24 hours after each noise exposure, a double dose (2 weeks apart) of 100 dB noise (8–16 kHz) exposures to young (4-week-old) CBA mice resulted in no permanent threshold shifts (PTS) and abnormal distortion product otoacoustic emissions (DPOAE). However, although auditory brainstem response (ABR) thresholds recovered fully in once- and twice-exposed animals, the growth function of ABR wave $1_{p\text{-}p}$ amplitude (synchronized spiral ganglion cell activity) was significantly reduced to a similar extent, suggesting that damage resulting from a second dose of the exposure was not proportional to that observed after the initial exposure. Estimate of surviving inner hair cell afferent terminals using immunostaining of presynaptic ribbons revealed ribbon loss of ~40 % at the ~23 kHz region after the first round of noise exposure, but no additional loss of ribbons after the second exposure. In contrast, a third dose of the same noise exposure resulted in not only TTS, but also PTS even in regions where DPOAEs were not affected. The pattern of PTS seen was not entirely tonotopically related to the noise band used. Instead, it resembled more to that of age-related hearing loss, i.e., high frequency hearing impairment towards the base of the cochlea. Interestingly, after a 3rd dose of the noise exposure, additional loss of ribbons (another ~25 %) was observed, suggesting a cumulative detrimental effect from individual "benign" noise exposures, which should result in a significant deficit in central temporal processing.

Keywords: auditory, noise-induced hearing loss, temporary threshold shift, CBA mice

INTRODUCTION

Prior noise exposures can exacerbate age-related hearing loss (Kujawa and Liberman 2006). Surprisingly, a noise exposure previously believed to be "benign" has been shown to cause irreversible neural damages in the absence of elevated hearing thresholds (Kujawa and Liberman 2009; Lin et al. 2011), raising the question as to whether cochlear aging may be a function of cumulative prior overexposures which may not manifest in dramatic permanent threshold shifts (PTS) after a single noise exposure. In mice exposed with an octave-band noise that causes maximally temporary threshold shift (TTS), Kujawa and Liberman (2009) have reported the following observations: (1) fully recovered hearing thresholds measured with evoked auditory brainstem responses (ABR), (2) normal distortion product otoacoustic emissions (DPOAE), (3) total preservation of mechanosensory hair cells (both inner and outer), and (4) massive spiral ganglion cell (SGC) afferent terminal

Correspondence to: Yong Wang · Division of Otolaryngology and Program in Neuroscience · University of Utah · 30 North, 1900 East, Salt Lake City, UT 84132-0002, USA. Telephone: +1-801-5873846; fax: +1-801-5855744; email: yong.wang@hsc.utah.edu

damage and retraction under the inner hair cell (IHC). Retraction of type I SGC afferent terminals starts immediately after the noise overstimulation, with the formation of vacuoles under the IHC (Puel et al. 1998; Wang et al. 2002). More than 50 % of the afferent fibers can be affected after a single noise exposure, and retract to the first semi-node of Ranvier where they appear stabilized for many months before a delayed neuronal degeneration (Kujawa and Liberman 2009; Lin et al. 2011). Other acute histopathology changes after a TTS noise exposure include: ganglion cell demyelination (Wang et al. 2002), buckling of the pillar cell bodies (Nordmann et al. 2000), collapse of outer Nuel's spaces (Wang et al. 2002), and severe loss of type IV fibrocytes in the spiral ligament (Adams 2009; Wang et al. 2002). Although certain non-neural elements (e.g., pillar cells, Nuel's space) recover fully along with the thresholds within 2 weeks (Nordmann et al. 2000; Wang et al. 2002), the loss of type IV fibrocytes is irreversible (Adams 2009; Wang et al. 2002). The growth of ABR wave $1_{p\text{-}p}$ amplitude (summed SGC activity) as a function of increasing sound intensity is greatly reduced even after the full recovery of ABR thresholds, consistent with the observed auditory nerve afferent terminal damage (Kujawa and Liberman 2009; Lin et al. 2011). Intact afferent terminals may be important for the preservation of hearing sensitivity. During age-related hearing loss, morphologic alterations of IHC synaptic terminals precede the loss of spiral ganglion cells and hearing sensitivity (Stamataki et al. 2006). Furthermore, survival of the spiral ganglion cells requires the attachment of afferent terminals to the IHC ribbon synapses; postsynaptic SGCs do not survive when ribbon synapses are disrupted (Seal et al. 2008). To test the consequences of repeated TTS noise exposures, we examined physiological and histological changes of the inner ears in young CBA mice after a single or multiple doses of TTS noise exposure.

MATERIALS AND METHODS

Animals

CBA/CaJ mice of either sex at 4 weeks old were entered into the study. The mice were originally obtained from the Jackson Laboratory (Bar Harbor, ME, USA) and subsequently maintained through in-house breeding. All experimental procedures were approved by the Institutional Animal Care and Use Committee at the University of Utah.

Noise exposures

Awake mice (two at a time) were placed inside a wire-mesh cage (7" × 7" × 3.5" with four partitions) suspended in a reverberant noise exposure box and exposed to the noise for 2 hrs, unanaesthetized and unrestrained. The noise was an octave-band noise centered at 12 kHz, and it was generated by a General Radio 1381 (Concord , MA, USA) or later by a Wavetek model 132 (San Diego, CA, USA) random noise generator, filtered (bandpass, 8th order Butterworth, Rockland 2382; Rockleigh, NJ, USA), amplified (D-75 power amplifier; Crown Audio, Elkhart, IN, USA), and delivered (compression driver; JBL, Northridge, CA, USA) through an exponential horn aimed at the center of the reverberant chamber from the top. To achieve the maximum TTS noise exposure, the noise level was adjusted to 100±1 dB SPL, measured at the center of each partition within the cage. Sound pressure level was monitored constantly during the noise exposure with a 1/4" pressure microphone (ACO Pacific, Belmont, CA, USA) inserted in the suspended cage at the mouse ear level. Three groups of experimental animals, randomly assigned, received 1× (at P28), 2× (at P28 and P42), and 3× (at P28, P42 and P56) 100 dB exposures respectively. After each exposure, the animals were returned to their home cages in an isolated area in the housing facility with ambient noise level between 50–60 dB SPL.

ABR and DPOAE testing

ABRs and DPOAEs were performed 1 day and 2 weeks after each noise exposure (Fig. 1) or as indicated. Mice were anesthetized with a combination drug of ketamine (100 mg/kg) and xylazine (10 mg/kg i.p.). ABRs/DPOAEs were done in a double-walled sound chamber (IAC, Bronx, NY, USA). The body temperature was maintained at ~37 °C via a heating lamp. Only the right ear from each animal was tested. A small incision was made at the tragus to allow better access to the ear canal. For ABRs, an electrostatic speaker (EC-1, Tucker–Davis Technology, Alachua, FL, USA) fitted with a 1.5-cm-long polyethylene tube was placed abutting the ear canal. Recording electrodes were placed under the skin at the vertex and mastoid, with a remote ground in the rump area. ABR signals were amplified with a TDT RA4 pre-amplifier, filtered from 100 to 3,000 Hz, averaged and digitized with a TDT RA16BA processor controlled by BioSigRP software. Acoustic stimuli were digitally generated and processed by a RX6 real-time processor, and passed through a PA5 attenuator prior to delivery to the speaker amplifier at a rate 24–32 times/sec. A series of responses to either clicks (0.1 ms) or tone pips (5 ms with 0.5 ms $\cos^2$ rise and fall) were collected with 5 or 10 dB intensity steps, over a 70–80 dB range. Click polarities were alternated on sequential trials, and the waveforms averaged to minimize cochlear microphonics. ABR traces were visually inspected after plotting the amplitude of each peak against stimulus intensity. Two independent observers estimated the

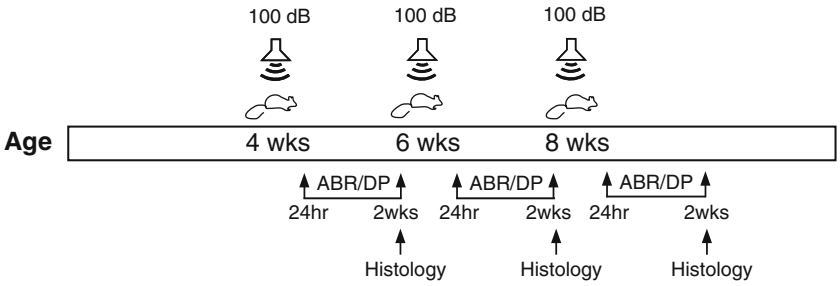

FIG. 1. Timeline of experimental procedures. Animals entered into experiments at 4 weeks of age and exposed to a 100 dB SPL octave-band noise once, twice or triple times depending on the group assignment. Animals were allowed 2 weeks time to recover from the prior exposure. ABR and DP measurements were performed at 24 hrs (TTS) and 2 weeks (PTS) after each noise exposure.

threshold as the lowest intensity at which the response was clearly discernable. Thresholds typically corresponded to a level one step below that at which the peak-to-peak response amplitude began to rise. The DPOAEs were measured using an ER-10B+(Etymotic Research) microphone coupled with two EC1 speakers. Stimuli of two primary tones f_1 *and* f_2 (f_2/f_1 =1.2) were presented with $f_2=f_1-10$ dB. Primary tones were stepped from 30 to 80 dB SPL (for f_1) in 10 dB increment and swept from 8 to 32 kHz in ½ octave steps. Stimuli were generated and attenuated digitally (200 kHz sampling). The ear canal sound pressure was preamplified and digitized. A fast Fourier transformation was computed, and the sound pressures at f_1, f_2, and $2f_1$- f_2 were extracted after spectral averaging from 50 serial waveform traces (each corresponding to 84 ms of digitized ear canal sound pressure waveform). The noise floor (average of ten points in the FFT on either side of $2f_1$-f_2) was also measured: it ranged between −25 and 0 dB SPL, depending on the test frequencies. All data were shown in mean ± SEM.

Immunohistology and confocal imaging

Animals were perfused intracardially with freshly prepared 4 % paraformaldehyde following the designated 2-week post noise exposure tests. Both temporal bones were dissected out, and the round and oval windows opened to allow efficient diffusion of the fixative into the labyrinth. After overnight post-fixation in the same fixative at 4°C, the temporal bones were decalcified in 0.1 M EDTA at 4 °C for at least 3 days. The entire decalcified cochlea was then microdissected into three sections of roughly equal size, and immunostained with mouse anti-$CtBP_2$ (C-terminal binding protein 2, BD Biosciences) at 1:200 dilution. AlexaFluro 488 conjugated goat anti-mouse IgG secondary antibody (1:500, Invitrogen) was used to visualize positive $CtBP_2$ immunostaining. The stained cochlear sections were carefully separated from the decalcified bony shell and mounted on slides in Fluoromount (Sigma). Cochlear frequency location was mapped using a place to frequency relationship formula $d\,(\%)=156.5-82.5\times\log(f)$, where d is percent distance from the base and f is the frequency in kHz (Muller et al. 2005). Ribbon synapses were imaged on an Olympus FV1000 confocal microscope. Z-series of the basal pole of the inner hair cells (~30 μm) were imaged with a 63× oil immersion objective in 1-μm steps. Ribbon counts per IHC were made by using a high N.A. 40× objective on a Zeiss microscope. We first localized the ~23 kHz region and selected a continuous stretch of 20–30 IHCs. All stained ribbons encompassing the whole synaptic pole of the IHCs in the selected region were counted, and the total count of ribbons in the region was then divided by the number of IHCs selected to obtain the ribbons/IHC estimate.

Histology and cytocochleogram

Animals were perfused intracardially after final physiological tests, and both temporal bones harvested as described above. After overnight fixation at 4 °C, cochleas were osmicated (1 % OsO_4 in distilled H_2O) for 60 min, and decalcified (0.1 M EDTA with 0.2 % glutaraldehyde). Following decalcification, cochleas were dehydrated in graded ethanol concentrations and propylene oxide, and then embedded in Araldite 502 resins and sectioned in a roughly horizontal plane parallel to apical modiolus in 50-μm thickness with a carbide steel knife. Cut sections were then mounted in Histomount (Ted Pella, Redding, CA, USA) on slides and coverslipped. A standard cytocochleogram was prepared for each ear using a 40× objective and Nomarski DIC optics on a Zeiss Axioskop. In each section through the cochlear duct, the number of present and absent hair cells was assessed throughout the entire section thickness (50 μm) and plotted as fractional survival (Wang et al. 2002). Evaluation of both the nuclear and cuticular regions was used to make these assessments.

RESULTS

We first determined the age of our experimental animals at which ABR waveforms and thresholds became fully developed and stabilized. As shown in Fig. 2, ABR waveforms (Fig. 2A) and thresholds (Fig. 2B) reached "mature-like" appearance and values at 3 weeks of age. Even though ABRs could be measured in 2-week-old CBA mice, the ABR waveforms were not fully developed, and the thresholds were uniformly elevated >for ~30 dB across the tested frequencies, consistent with

the development timeline for cochlear amplification in mice (Song et al. 2008). Since the ABR thresholds (Limb and Ryugo 2000) and vulnerability of CBA mice to noise overexposures (Kujawa and Liberman 2006) remain relatively constant before 10 weeks of age, we chose to start the noise exposure when the mice turned 4 weeks old.

ABR thresholds and DPOAEs after TTS noise exposures

We measured temporary hearing threshold shifts 24 hours after each 100-dB noise exposure, and found that the amount and pattern of threshold elevation were very similar after the 1st, the 2nd, and even the 3rd 100 dB noise exposure (Fig. 3A, $p>0.05$, $n=8–11$). The peak threshold shift was 30–40 dB at ~23 kHz, very similar to previous reports of TTS with similar octave band noise (Hirose and Liberman 2003; Kujawa and Liberman 2009; Wang et al. 2002). This amount of TTS was not at the saturation level, and recovered fully within 2 weeks time (Fig. 3B and inset, $p>0.05$, $n=8–16$) for once and twice noise-exposed animals, but not for thrice noise-exposed animals, which showed worsening threshold elevation at frequencies above 11 kHz 2 weeks after the 3rd exposure (threshold $\Delta=6.1\pm1.6$ dB @11.3 kHz, 11.9 ± 2.2 dB @16 kHz, 17.4 ± 2.6 dB @22.6 kHz, 18.8 ± 4.6 dB @32 kHz, and 25.1 ± 3.3 dB @45.2 kHz, $p<0.01$ for all pairwise frequency comparisons, Fig. 3B). Nevertheless, it was possible to maintain the recovered ABR thresholds for at least 8 weeks post exposure after the 2nd 100-dB TTS noise exposure (Fig. 3B, also see Kujawa and Liberman 2009). As a comparison, the same octave-band noise at 106 dB SPL delivered once produced not only larger temporary threshold shift (Fig. 3A), but also permanent threshold shift 2 weeks post exposure at the tonotopically appropriate region ($n=7$, Fig. 3B). We also exposed animals once with the noise level at 103 dB SPL, which resulted in intermediate PTS between 100 dB and 106 dB noise-exposed animals (Fig. 3B). Thus it appeared that our 100 dB SPL noise exposure represented a condition that produced maximal TTS without causing significant PTS in young CBA mice.

A dominant component of the TTS at 24 hrs was a severe reduction of DPOAEs (measured in a subset of animals) after each noise exposure, as shown in Fig. 3C. However, DPOAEs returned to normal levels 2 weeks after each exposure in 1× and 2× noise-exposed animals at 16 kHz, 22.6 kHz, and 32 kHz ($p>0.05$, $n=6$, two-way ANOVA). For the 3rd noise exposure, no loss of DPOAEs was detected at 16 kHz ($p>0.05$), however, there was some small reduction (<10 dB) of DPOAEs at 22.6 kHz ($p<0.01$, 2-way ANOVA, but $p>0.05$ for all post-hoc pairwise comparison with preexposure levels) and 32 kHz ($p<0.001$, with significant pairwise post hoc comparison only at 70 and 80 dB levels).

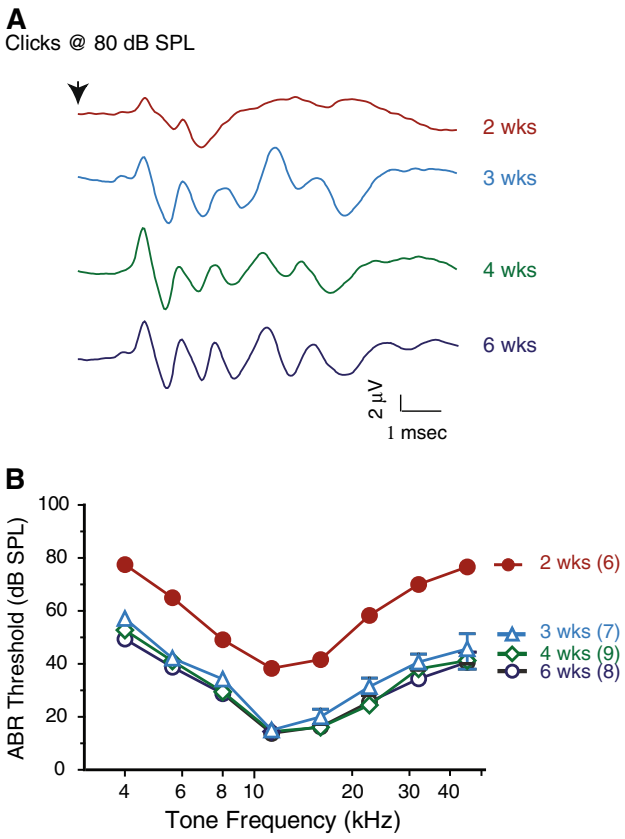

FIG. 2. Maturation of ABR waveform and thresholds. **A** Representative ABR waveforms to 80 dB SPL clicks from individual animals in different age groups. **B** ABR thresholds for animals of different ages. Threshold values reached adult level and stabilized after the mice turned 3 weeks old. There was no significant difference of ABR thresholds between different age groups (≥3 weeks). *Numbers inside the parentheses* indicate animal numbers in each group (hereafter).

Reduction of ABR wave 1 amplitude after TTS noise exposures

Even though ABR thresholds recovered fully 2 weeks after the 1x100 dB noise exposure, the ABR wave peaks of different latencies appeared less distinctive (Fig. 4A), suggesting less synchrony of summed activities at different stages of central auditory processing. Quantification of wave $1_{p\text{-}p}$ growth at 16 kHz, 23 kHz and 32 kHz, the frequencies where the biggest temporary threshold shifts were seen, showed significant reduction in wave $1_{p\text{-}p}$ amplitude at all suprathreshold levels ($p<0.0001$, $n=8–13$ per group, Fig. 4B). There was little additional reduction of wave $1_{p\text{-}p}$ amplitude in double-exposed group compared to the single-exposed group ($p>0.05$). The amount of wave $1_{p\text{-}p}$ reduction was roughly 50 % of the control values across all suprathreshold levels in both single- and double-exposed groups (Fig. 4B right panel). In contrast, a further

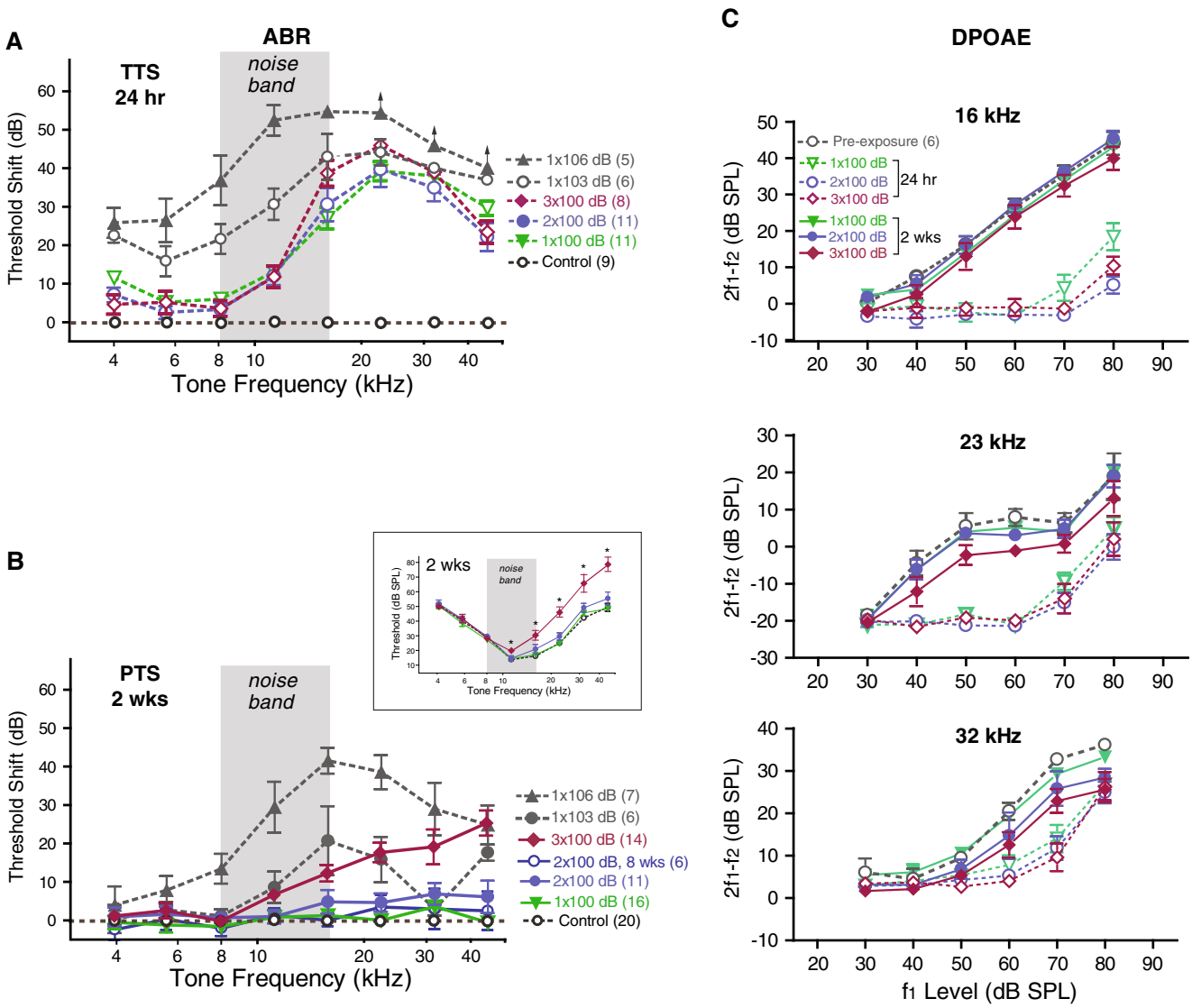

FIG. 3. ABR threshold shift. **A** Threshold shift measured 24 hrs after each noise exposure. There were no statistical differences between once, twice, and thrice noise-exposed groups. As comparison, both 103 dB and 106 dB noise-exposed animals showed larger TTS over a wider frequency range. *Arrows* in 106 dB group indicate measurement saturation. **B** Permanent threshold shift measured 2 weeks or 8 weeks after the noise exposure. *Inset:* absolute ABR thresholds 2 weeks post 1×, 2×, and 3× noise exposures. ABR thresholds at 11, 16, 23, 32, and 45 kHz were significantly elevated after the 3rd 100 dB noise exposure (ANOVA, $p<0.001$). * denotes $p<0.01$ post-hoc pairwise comparison to control. **C** DPOAEs at 16, 23 and 32 kHz measured prior to noise exposures and 24 hr and 2 weeks after each 100 dB noise exposures (a subset of animals as in **B**).

reduction of ~25 % in wave $1_{p\text{-}p}$ amplitude was observed in 3× 100 dB noise-exposed animals ($p<0.01$), which was accompanied by permanent threshold shift (Fig. 3B).

Loss of IHC-afferent synaptic ribbons

To correlate the reduction of suprathreshold ABR amplitudes to the loss of IHC-afferent terminals after the noise exposure(s), we quantified the afferent synaptic ribbons as described by Kujawa and Liberman (2009). Presynaptic ribbons can be visualized by using an antibody against $CtBP_2$ (C-terminal binding protein-2, a transcription factor sharing a homologous domain with the ribbon protein Ribeye). In general, there is a good correlation between presynaptic ribbon staining and post-synaptic receptor staining (Khimich et al. 2005; Meyer et al. 2009; Liberman et al. 2011; but see Kujawa and Liberman 2009; Lin et al. 2011). We estimated the number of synaptic ribbons per inner hair cell in tonotopically affected region of ~23 kHz. As suggested by ABR physiological data, the loss of ribbon synapses was very similar between 1× and 2× 100 dB noise-exposed groups. The IHC ribbon densities at the ~23 kHz region were 14.4±0.8, 8.7±1.1, and 9.6±0.8 ribbons/IHC for control, 1×, and 2× noise-exposed groups respectively (one-way ANOVA with post-hoc pairwise comparisons; $p<0.01$ for either control vs 1× 100 dB or control vs. 2× 100 dB, but $p=0.53$ for 1× vs 2× 100 dB, $n=4$–5 ears in

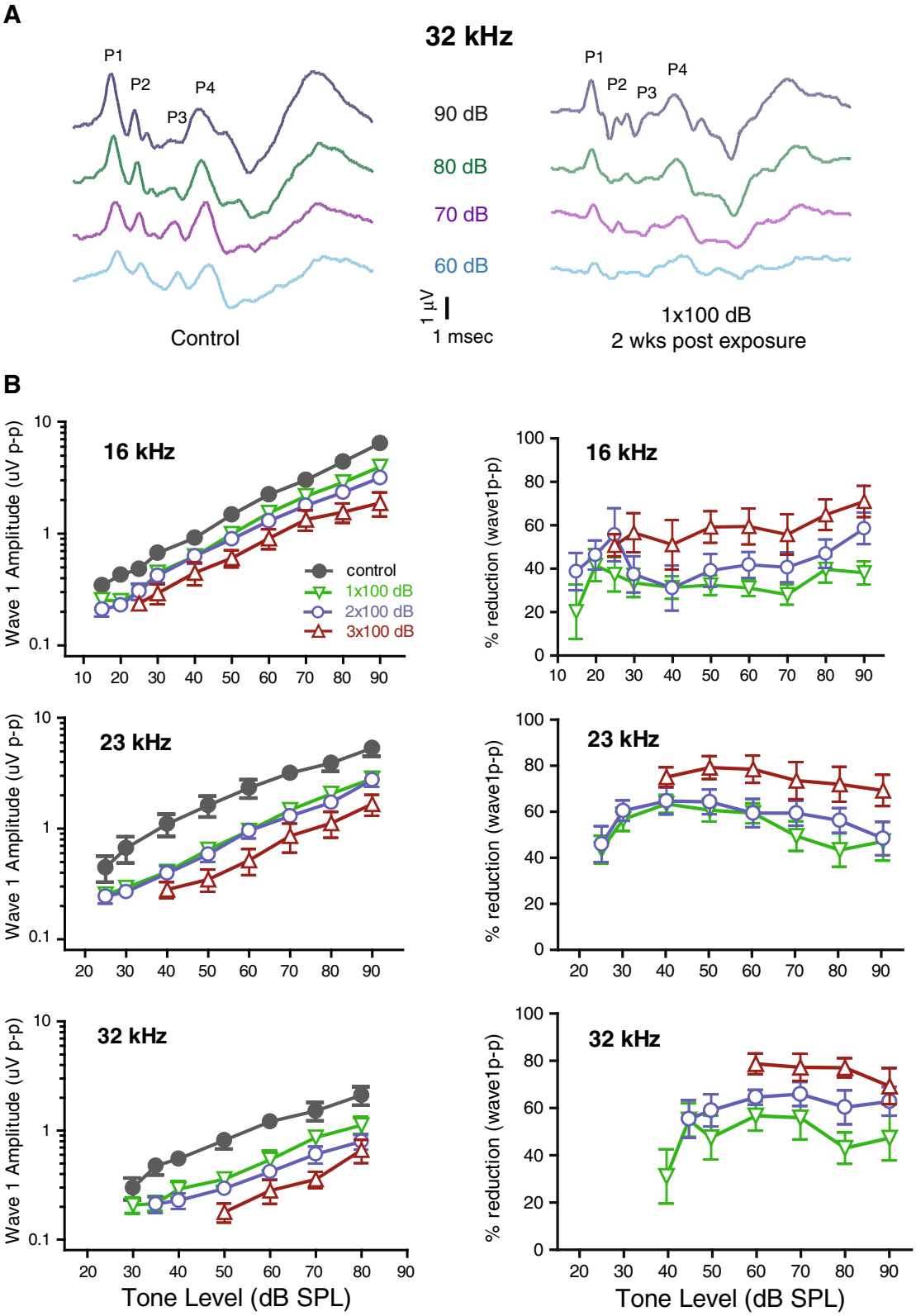

FIG. 4. Reduction of ABR wave $1_{p\text{-}p}$ amplitude. **A** Representative suprathreshold ABR responses to 32 kHz tone stimuli at varying intensities. *Left*: control; *right*: 1× 100 dB noise-exposed. Major positive peaks on the ABR waveforms are indicated. **B** *Left:* growth of ABR wave $1_{p\text{-}p}$ amplitude at 16, 23, and 32 kHz as a function of sound pressure level from control (unexposed), 1×, 2×, and 3× 100 dB noise-exposed animals. Wave$1_{p\text{-}p}$ amplitude reduction was comparable between 1× and 2× noise-exposed animals; however, there was a further reduction of wave $1_{p\text{-}p}$ amplitude after a 3rd 100 dB noise exposure. *Right:* percentage reduction of Wave $1_{p\text{-}p}$ amplitude was calculated as $(1 - W1_{p\text{-}p(noise)}/W1_{p\text{-}p(control)})$ and plotted to show the relative reduction of suprathreshold Wave $1_{p\text{-}p}$ amplitude.

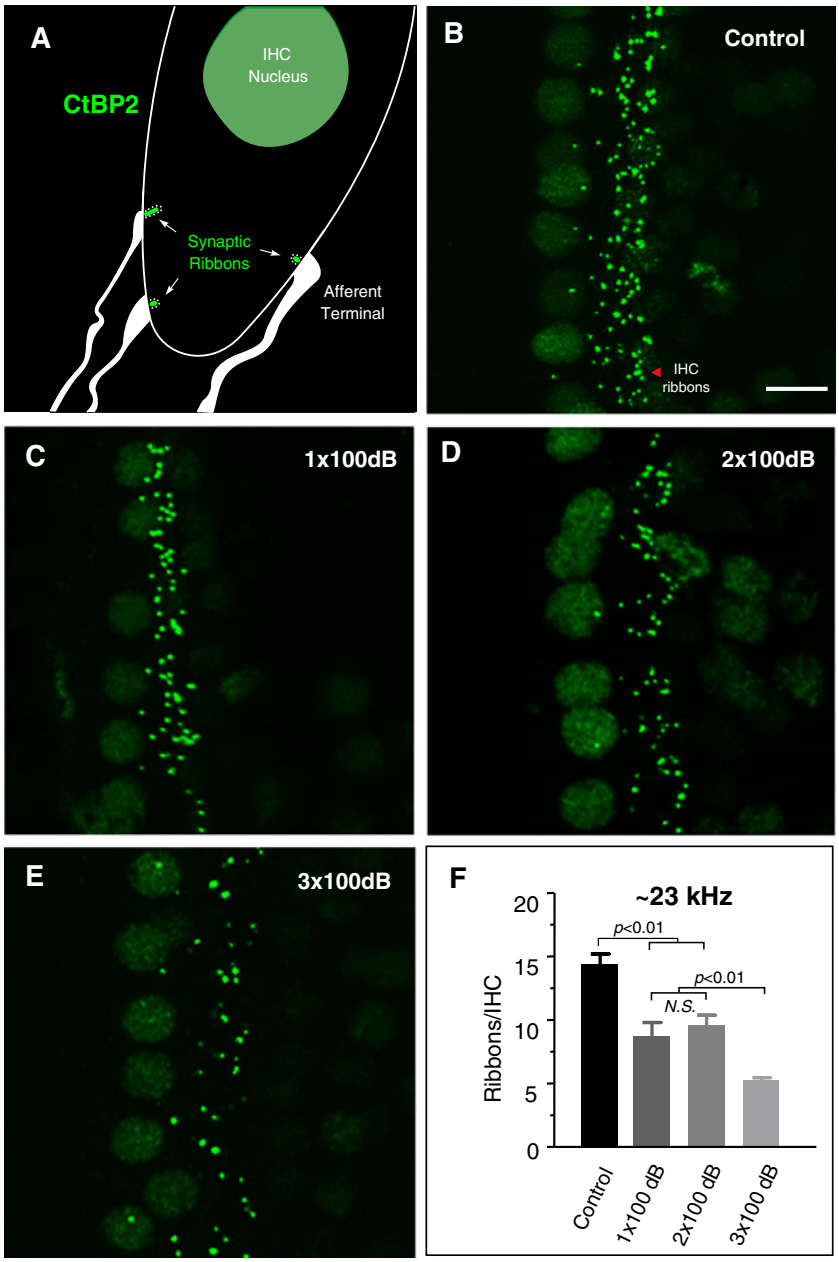

FIG. 5. Immunostaining of IHC synaptic ribbons with anti-$CtBP_2$. **A** Schematic diagram of the IHC basal pole depicting presynaptic ribbons (*green*) and apposed postsynaptic afferent terminals. **B-E** Representative images of positively stained synaptic ribbons from control, 1×, 2×, and 3× 100 dB noise-exposed animals. The images were reconstructed from z-projections encompassing the IHC terminal poles of ~30 μm thickness. *Scale bar* (10 μm) applies to **B-E**. **F** Quantification of ribbons per IHC at the ~23 kHz cochlear region. The IHC ribbon densities were 14.4±0.8, 8.7±1.1, and 9.6±0.8 ribbons/IHC respectively for control, 1×, and 2× 100 dB noise-exposed groups. There was a significant reduction of synaptic ribbons after 1× and 2× noise exposures compared to control (one-way ANOVA with post-hoc pairwise comparisons; $p<0.01$, $n=4–5$ ears in each group). The loss of synaptic ribbons were comparable between 1× and 2× 100 dB noise-exposed groups ($p=0.53$). A further loss of synaptic ribbons was seen after the 3rd 100 dB noise exposure (5.3±0.2 ribbons/IHC; $p<0.01$ between 3× 100 dB and all other groups) when PTS was also present at 23 kHz. Panel A adapted with permission from Lin et al. 2011

each group). A further reduction of ribbon synapses was observed after the 3rd 100 dB noise exposure (5.3±0.2 ribbons/IHC) when PTS was observed ($p<0.01$ between 3× 100 dB and all other groups). There was no apparent loss of outer hair cell ribbon synapses by the 100 dB noise exposure(s) (Fig. 5B-E).

Hair cell loss and cochlear histology

Histopathology examination of the organ of Corti at ~23 kHz region showed largely normal histological appearance with no loss of either IHCs or OHCs in 1×, 2×, and even for 3× 100 dB noise-exposed animals (Fig. 6). Even though there was some loss of OHCs at the extreme base of the cochleas after 3× 100 dB exposures (Fig. 6E), the occurrence of such OHC loss at the cochlear base was found in only half of the ears examined (three out of six). We found no evidence of spiral ganglion cell body loss in the time period studied (not shown, also see Kujawa and Liberman 2009). However, a severe loss of type IV fibrocytes in the spiral ligament was present in all noise-exposed groups (arrowheads, Fig. 6B–D).

DISCUSSION

Noise overexposures at an earlier age have long-term consequences on hearing in the life span of an animal (Kujawa and Liberman 2006, 2009). Here, we showed

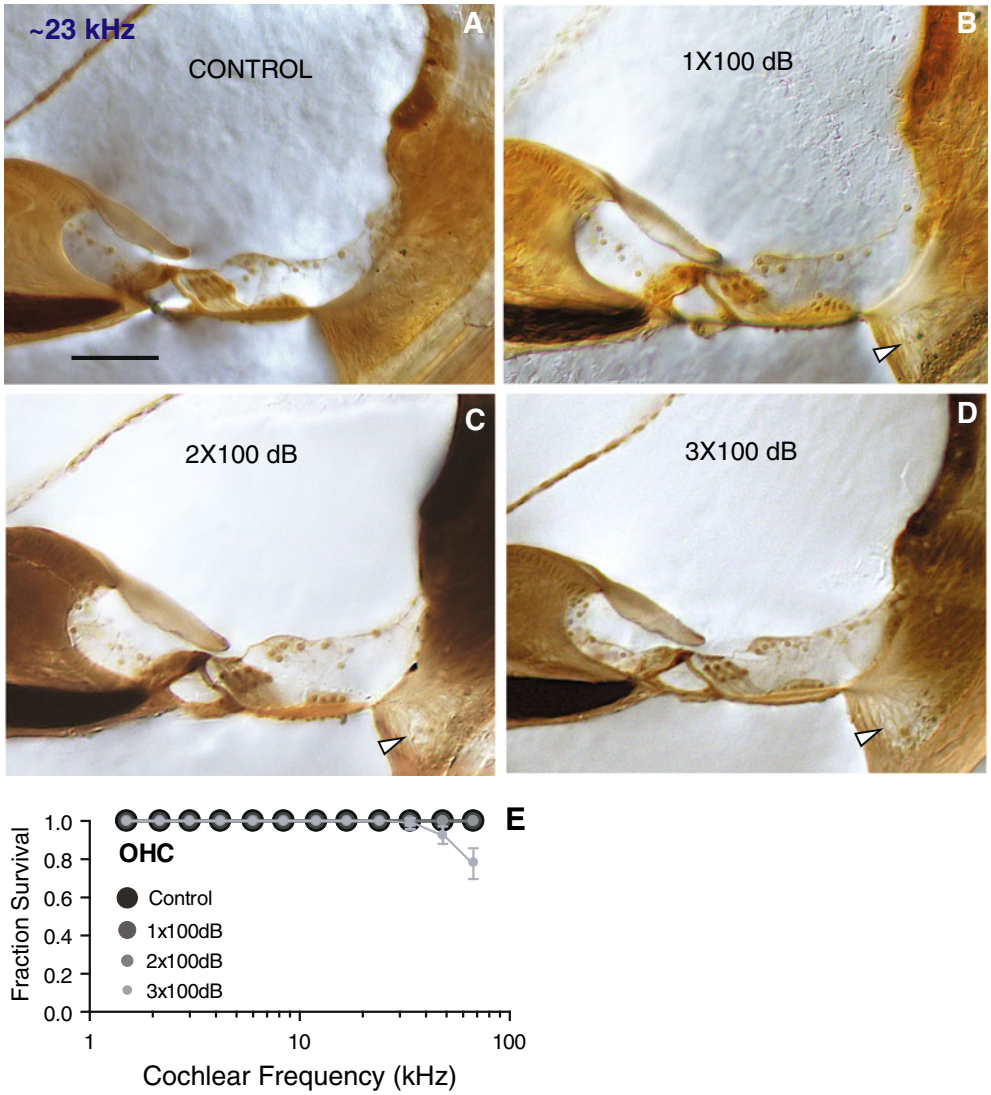

FIG. 6. Cross sections of the inner ear at ~23 kHz and a cytocochleogram. **A-D** Representative photographs of organ of Corti from individual animals in control, 1×, 2×, and 3× 100 dB noise-exposed groups 2 weeks post exposure. The only histological deficit under light microscopy was a severe loss of type IV fibrocytes in the spiral ligament, which was observed in all noise exposed groups (*arrowheads*). All other structures appeared normal. *Scale bar* (50 μm) applies to **A-D**. **E** Cytocochleogram showed some loss of outer hair cells at the extreme base of the cochlea from 3× 100 dB noise-exposed group, but that was only in three of six ears examined.

that two sequential doses of maximal TTS exposure resulted in no or little permanent ABR threshold elevation. However, a third dose of the same noise exposure resulted in significant hearing threshold shift at the high frequency region, despite a similar pattern of temporary threshold shift at 24 hrs post-exposure. The pattern of the PTS induced with the repetitive TTS noise exposures was reminiscent of the age-related hearing loss (Willott and Erway 1998). Since detachment of afferent terminals from the inner hair cells was widespread (from the tonotopic location to the extreme cochlear base) and the onset of ganglion cell death was delayed after a TTS noise exposure (Kujawa and Liberman 2009; Lin et al. 2011), the PTS we observed at 16 kHz and above after the 3rd TTS noise exposure could be linked to the cumulative afferent terminal damages caused by multiple noise exposures. This was supported by the observation that there was no loss of DPOAEs (at least @16 kHz region), but there was additional loss of IHC-afferent terminals (total ~70 %) after the 3rd noise exposure, compared to ~40 % ribbon synapse loss in once and twice exposed animals.

Relevance to age-related hearing loss

The observation that cumulative TTS noise exposures induced an aging-like hearing loss rather than a distinctive, tonotopically appropriate threshold shift more commonly seen in noise-induced hearing loss (Wang et al. 2002) suggests that qualitatively different neural and structural elements may be damaged at

different cochlear locations between TTS and PTS noise exposures. In CBA mice, the band noise used seems to induce cochlear histopathology at two loci: tonotopic and the hook region (Wang et al. 2002). Although excitotoxicity (e.g., synaptic terminal vacuoles) is seen at the tonotopic region in both TTS and PTS noise-exposed ears, strial edema and IHC stereocillia disarray/fusion are only associated with PTS at the tonotopic location (Liberman and Dodds 1984b; Robertson 1982; Wang et al. 2002). Many factors have been suggested to contribute to age-related hearing loss, including: type IV fibrocytes in the spiral ligament (Adams 2009; Hequembourg and Liberman 2001) and chronic reduction of endocochlear potential (EP) (Lang et al. 2010). Type IV fibrocytes in the spiral ligament appear to be highly sensitive to noise exposures (Adams 2009; Wang et al. 2002). Loss of type IV fibrocytes at the cochlear base is always observed in noise induced hearing loss regardless of the noise spectrum (Adams 2009). Moreover, histopathologic changes of type IV fibrocytes at the hook region precede the onset of physiological hearing threshold shift during age-related hearing loss (Hequembourg and Liberman 2001). However, hearing thresholds can recover fully at regions without repopulation of type IV fibrocytes, e.g., at ~23 kHz, which seems to indicate that type IV fibrocytes may not be as critical in maintaining hearing sensitivity. Chronic loss of EP has been proposed recently as a major factor in age-related hearing loss (Lang et al. 2010; but see Hirose and Liberman 2003). It is not clear it can fully account for the hearing loss, because the EP loss is fairly uniform in the cochlear duct, while the threshold elevation has a typical high frequency emphasis.

IHC afferent terminal loss encompasses areas from the extreme base of the cochlea to the tonotopic locus with only a single dose of TTS noise exposure (Kujawa and Liberman 2009; Lin et al. 2011). Incremental loss of afferent terminals was observed when PTS occurred (Figs. 3, 4, and 5). Can this additional afferent terminal loss seen in 3× noise-exposed animals account for the threshold shift? Assuming a contribution of 100 nV per auditory nerve fiber to the compound action potential (CAP) (Prijs 1986), CAP threshold at 20–30 kHz in mice is ~5 μV (Yoshida and Liberman 2000; Wang and Liberman 2002), which would require ~50 low threshold ANFs. This translates to about six IHCs, assuming 15 ANFs per IHC, and 60 % of these fibers are high SR (spontaneous rate >5 sp/sec), low threshold fibers (Taberner and Liberman 2005). An increase of 5 dB sound level would recruit an additional ten IHC based on Q_{10dB} of 6 at 20 kHz (Taberner and Liberman 2005), cochlear length 5.2 mmm (1.25 mm/octave) (Muller et al. 2005), and 750 IHCs/cochlea (Wang et al. 2002). Thus, even with a loss of ~40 % of afferent fibers (assuming all low threshold fibers, which is unlikely) after 1× and 2× TTS noise exposures, 16 IHCs are left with ~144 afferent fibers, among which ~50 should be low-threshold fibers. With the additional loss of 25 % afferent terminals after the 3rd TTS noise exposure (Fig. 5F), the survival number of low threshold fibers should fall (well) below the 50 required to keep the threshold within 5 dB of the normal level. We noted that our ribbon counts per IHC are slightly lower (though not significant) than those previously reported (Kujawa and Liberman 2009; Meyer et al. 2009), which may stem from differences in methodology. Normal thresholds can be maintained even when ribbon count is reduced to ~7 synapses/IHC (Kujawa and Liberman 2009), however, PTS is associated with ribbon count at ~5 synapses/IHC (Fig. 5B). This steepness of threshold elevation may reflect the switching from low-threshold fibers to high-threshold fibers as major contributors to the threshold. Can OHC distortion products loss account for observed permanent ABR threshold shift? Clearly, a dominant factor in TTS was the loss of DPOAEs, as evidenced when DP was measured 24 hrs after each noise exposure (Fig. 3C). However, DPOAEs were essentially fully recovered by 2 weeks post exposure. Compellingly, at the 16 kHz region, there was no abnormality in DPOAEs even after the 3rd noise exposure. Moreover, even at 23–32 kHz regions the amount of ABR threshold shift (~20 dB) is greater than the reduction of DPOAEs (<10 dB) observed after the 3rd noise exposure, indicating other neural elements must contribute to the ABR threshold shift manifested. It is likely that loss of DP (Fig. 3C) and OHCs (Fig. 6E) contributed to the worsening of threshold elevation towards the cochlear base. Taken together, threshold elevation at the tonotopical locus matches well with the afferent ribbon loss observed, and accumulation of afferent terminal damage over time with recurrent noise exposures could be a major contributor to age-related hearing loss.

As a side note, we did not observe any beneficial effects of prior acoustic exposure(s) in reducing the effect of subsequent noise overexposures (Canlon and Fransson 1998; Yoshida and Liberman 2000), since the TTS from the subsequent noise exposure was not reduced compared to the first round of exposure (Fig. 3A). This is not surprising, since the protective effect of prior noise conditioning may be due to the protective effect of systemic stress response, and that has a narrow time window of effectiveness (Wang and Liberman 2002; Yoshida et al. 1999).

Vulnerability of afferent terminals

We observed a significant reduction in ABR wave $1_{p\text{-}p}$ growth function in single dose exposed animals

(Kujawa and Liberman 2009; Lin et al. 2011). Unexpectedly, we did not see worsening of ABR wave $1_{p\text{-}p}$ amplitude growth when comparing one dose to two doses of 100 dB overexposure, suggesting that, in naïve animals, the high-threshold fibers (with low SR) or a subset of low-threshold (with high SR) neurons (Liberman 1982; Liberman and Dodds 1984a) may be more susceptible to noise insults. In cats and guinea pigs, there seem to be a segregation of afferent terminal distribution, where low SR, high-threshold fibers are found more often on the modiolus side, whereas high SR, low-threshold fibers are often found on the pillar cell side of the inner hair cell (Liberman 1982; Tsuji and Liberman 1997). More recent studies suggest this segregation may be more likely on a basal to apical axis of the IHC (Liberman et al. 2011; Lin et al. 2011). Our study did not reveal obviously preferential loss of ribbons on the pillar/apical side vs modiolar/basal side, although the existence of such SR-based IHC-afferent terminal distribution is yet to be defined in mice. Nevertheless, if the low-threshold, high SR fibers were more vulnerable, a subclass of these fibers must be somewhat more resistant to acoustic insults, and are able to survive to allow hearing thresholds to recover after the 1st and 2nd 100 dB noise exposure. It is not clear what allows these type I afferent fibers to be more resistant to noise overexposures. It would be interesting to learn if these "tough" fibers have a high level of efferent innervation (Darrow et al. 2006, 2007). Nevertheless, there is a second wave of afferent terminal loss, which can accompany elevation of hearing thresholds. Simultaneous ribbon synapse pre- and post-staining has revealed that presynaptic $CtBP_2$ staining can overestimate the existence of postsynaptic structures (Kujawa and Liberman 2009; Lin et al. 2011). Therefore, the actual number of attached postsynaptic afferents may be even less then indicated, especially after 3× 100 dB noise exposures. This massive amount of afferent terminal loss must have a severe consequence on central auditory processing.

ACKNOWLEDGMENTS

We thank Dr. A. Park and M. Pasker for comments and proofreading the manuscript. Dr. MC Liberman provided the original schematic drawing used in Fig. 5A. Supported by NIDCD R03DC008190

REFERENCES

ADAMS JC (2009) Immunocytochemical traits of type IV fibrocytes and their possible relations to cochlear function and pathology. J Assoc Res Otolaryngol 10:369–382

CANLON B, FRANSSON A (1998) Reducing noise damage by using a mid-frequency sound conditioning stimulus. Neuroreport 9:269–274

DARROW KN, SIMONS EJ, DODDS L, LIBERMAN MC (2006) Dopaminergic innervation of the mouse inner ear: evidence for a separate cytochemical group of cochlear efferent fibers. J Comp Neurol 498:403–414

DARROW KN, MAISON SF, LIBERMAN MC (2007) Selective removal of lateral olivocochlear efferents increases vulnerability to acute acoustic injury. J Neurophysiol 97:1775–1785

HEQUEMBOURG S, LIBERMAN MC (2001) Spiral ligament pathology: a major aspect of age-related cochlear degeneration in C57BL/6 mice. J Assoc Res Otolaryngol 2:118–129

HIROSE K, LIBERMAN MC (2003) Lateral wall histopathology and endocochlear potential in the noise-damaged mouse cochlea. J Assoc Res Otolaryngol 4:339–352

KHIMICH D, NOUVIAN R, PUJOL R, DIECK ST, EGNER A, GUNDELFINGER ED, MOSER T (2005) Hair cell synaptic ribbons are essential for synchronous auditory signalling. Nature 434:889–894

KUJAWA SG, LIBERMAN MC (2006) Acceleration of age-related hearing loss by early noise exposure: evidence of a misspent youth. J Neurosci 26:2115–2123

KUJAWA SG, LIBERMAN MC (2009) Adding insult to injury: cochlear nerve degeneration after "temporary" noise-induced hearing loss. J Neurosci 29:14077–14085

LANG H, JYOTHI V, SMYTHE NM, DUBNO JR, SCHULTE BA, SCHMIEDT RA (2010) Chronic reduction of endocochlear potential reduces auditory nerve activity: further confirmation of an animal model of metabolic presbyacusis. J Assoc Res Otolaryngol 11:419–434

LIBERMAN LD, WANG H, LIBERMAN MC (2011) Opposing gradients of ribbon size and AMPA receptor expression underlie sensitivity differences among cochlear-nerve/hair-cell synapses. J Neurosci 31(3):801–808. doi:10.1523/JNEUROSCI.3389-10.2011

LIBERMAN MC (1982) Single-neuron labeling in the cat auditory nerve. Science 216:1239–1241

LIBERMAN MC, DODDS LW (1984a) Single-neuron labeling and chronic cochlear pathology. II. Stereocilia damage and alterations of spontaneous discharge rates. Hear Res 16:43–53

LIBERMAN MC, DODDS LW (1984b) Single-neuron labeling and chronic cochlear pathology. III. Stereocilia damage and alterations of threshold tuning curves. Hear Res 16:55–74

LIMB CJ, RYUGO DK (2000) Development of primary axosomatic endings in the anteroventral cochlear nucleus of mice. J Assoc Res Otolaryngol 1:103–119

LIN HW, FURMAN AG, KUJAWA SG, LIBERMAN MC (2011) Primary neural degeneration in the Guinea pig cochlea after reversible noise-induced threshold shift. J Assoc Res Otolaryngol 12(5):605–616. doi:10.1007/s10162-011-0277-0

MEYER AC, FRANK T, KHIMICH D, HOCH G, RIEDEL D, CHAPOCHNIKOV NM, YARIN YM, HARKE B, HELL SW, EGNER A, MOSER T (2009) Tuning of synapse number, structure and function in the cochlea. Nat Neurosci 12:444–453

MULLER M, HUNERBEIN K, HOIDIS S, SMOLDERS JW (2005) A physiological place-frequency map of the cochlea in the CBA/J mouse. Hear Res 202:63–73

NORDMANN AS, BOHNE BA, HARDING GW (2000) Histopathological differences between temporary and permanent threshold shift. Hear Res 139:13–30

PRIJS VF (1986) Single-unit response at the round window of the guinea pig. Hear Res 21:127–133

PUEL JL, RUEL J, D'ALDIN CG, PUJOL R (1998) Excitotoxicity and repair of cochlear synapses after noise-trauma induced hearing loss. Neuroreport 9:2109–2114

ROBERTSON D (1982) Effects of acoustic trauma on stereocilia structure and spiral ganglion cell tuning properties in the guinea pig cochlea. Hear Res 7:55–74

SEAL RP, AKIL O, YI E, WEBER CM, GRANT L, YOO J, CLAUSE A, KANDLER K, NOEBELS JL, GLOWATZKI E, LUSTIG LR, EDWARDS RH (2008)

Sensorineural deafness and seizures in mice lacking vesicular glutamate transporter 3. Neuron 57:263–275

Song L, McGee J, Walsh EJ (2008) Development of cochlear amplification, frequency tuning, and two-tone suppression in the mouse. J Neurophysiol 99:344–355

Stamataki S, Francis HW, Lehar M, May BJ, Ryugo DK (2006) Synaptic alterations at inner hair cells precede spiral ganglion cell loss in aging C57BL/6J mice. Hear Res 221:104–118

Taberner AM, Liberman MC (2005) Response properties of single auditory nerve fibers in the mouse. J Neurophysiol 93:557–569

Tsuji J, Liberman MC (1997) Intracellular labeling of auditory nerve fibers in guinea pig: central and peripheral projections. J Comp Neurol 381:188–202

Wang Y, Hirose K, Liberman MC (2002) Dynamics of noise-induced cellular injury and repair in the mouse cochlea. J Assoc Res Otolaryngol 3:248–268

Wang Y, Liberman MC (2002) Restraint stress and protection from acoustic injury in mice. Hear Res 165:96–102

Willott JF, Erway LC (1998) Genetics of age-related hearing loss in mice. IV. Cochlear pathology and hearing loss in 25 BXD recombinant inbred mouse strains. Hear Res 119:27–36

Yoshida N, Kristiansen A, Liberman MC (1999) Heat stress and protection from permanent acoustic injury in mice. J Neurosci 19:10116–10124

Yoshida N, Liberman MC (2000) Sound conditioning reduces noise-induced permanent threshold shift in mice. Hear Res 148:213–219